Neuron, Vol. 14, 29–41, January, 1995, Copyright © 1995 by Cell Press

Mice Devoid of the Glial Fibrillary Acidic Protein Develop Normally and Are Susceptible to Scrapie Prions

Hiroshi Gomi,* Takashi Yokoyama,† Kazushi Fujimoto,‡ Toshio Ikeda,* Akira Katoh,* Takeshi Itoh,* and Shigeyoshi Itohara*
*Institute for Virus Research
Kyoto University
Syogo-in, Sakyo-ku, Kyoto 606-01
Japan
†National Institute of Animal Health
Kannon-dai, Tsukuba, Ibaraki 305
Japan
‡Department of Anatomy
Faculty of Medicine
Kyoto University
Yoshida, Sakyo-ku, Kyoto 606-01
Japan

Summary

Glial fibrillary acidic protein (GFAP) is an intermediate filament protein specifically expressed in astrocytes in the CNS. To examine the function of GFAP in vivo, the *Gfap* gene was disrupted by gene targeting in embryonic stem cells. Mice homozygous for the mutation were completely devoid of GFAP but exhibited normal development and showed no obvious anatomical abnormalities in the CNS. When inoculated with infectious scrapie prions, the mutant mice exhibited neuropathological changes typical of prion diseases. Infectious prions accumulated in brains of the mutant mice to a degree similar to that in control littermates. These results suggest that GFAP is not essential for the morphogenesis of the CNS or for astrocytic responses against neuronal injury. The results argue against the hypothesis that GFAP plays a crucial role in the pathogenesis of prion diseases.

Introduction

Intermediate filament (IF) proteins are prominent components of the cytoskeleton and nuclear envelope of most eukaryotic cell types. IF proteins constitute an extremely large multigene family and are classified into the distinct sequence types I–V (for review, see Steinert and Roop, 1988). The expression of IF proteins exhibits a high degree of cell-type specificity, such as keratins of types I and II in epithelial cells, neurofilaments of type IV in nerve cells, desmin of type III in muscle cells, vimentin of type III in various mesenchymal cells, and glial fibrillary acidic protein (GFAP) of type III in astrocytes (for a review, see Steinert and Roop, 1988). The differential expression of IF proteins in different cell types implies that they have specialized roles in the differentiation and function of these cells. The following evidence supports this concept. Injection of antibodies against neurofilament-M subunit into Xenopus laevis embryos inhibits development of peripheral nerve cells (Szaro et al., 1991). Transgenic mice that accumulate neurofilament-L subunit exhibit axonal degeneration and severe skeletal muscle atrophy (Xu et al., 1993). A mutant strain of the Japanese quail, *quiver*, which lacks neurofilaments, has the clinical feature of generalized quivering and the morphological feature of decrease in size of myelinated axons (Yamasaki et al., 1991). Keratin depletion in Xenopus embryos by either antisense oligonucleotides or antibody injection prevents gastrulation (Klymkowsky et al., 1983; Torpey et al., 1992). Transgenic mice expressing a dominant-negative form of keratin 14 suffered from skin abnormalities resembling a human genetic disease (Vassar et al., 1991). A null mutation in the keratin 8 gene, which is first expressed together with keratin 18 during embryogenesis, causes mid-gestational lethality in mice (Baribault et al., 1993).

Astrocytes fill the interstices between neuronal cell bodies and extend processes to ensheathe axons and blood vessels (Peters et al., 1991). Astrocytes are believed to be crucial for the nutritional and structural support of neurons and for the regulation of local concentrations of neurotransmitters and ions. Other studies suggest that astrocytes have an inductive role in the formation of tight junctions between brain endothelia (Janzer and Raff, 1987; Arthur et al., 1987), contributing to the establishment of the blood-brain barrier (BBB) in vivo. The function of GFAP in astrocytes is largely unknown. Interestingly, removal of GFAP in a human astrocytoma cell line by transfection with an antisense construct caused an impaired ability of the cells to extend glial processes upon neuronal induction (Weinstein et al., 1991), suggesting the necessity of GFAP for the formation of stable astrocytic processes in response to neurons. During development of the CNS, neurons are born on the ventricular surface of the neural tube and appear to migrate to their final destination along astrocytic processes (Rakic, 1972, 1981). Thus, it is predicted that structural support of astrocytic processes by GFAP may be critical for the morphogenesis of the CNS.

Astrocytes show remarkable cellular responses to a wide range of pathological conditions of the CNS. Astrocyte swelling, the Alzheimer type II response, and reactive astrocytosis (reactive gliosis) are examples of common astrocytic changes (for review, see Norenberg, 1994). Reactive astrocytes are characterized histologically by cytoplasmic hypertrophy associated with profusion of long and thick processes filled with GFAP, and by often enlarged and irregularly outlined nuclei. The astroglial scarring that frequently occurs under pathological conditions has also been interpreted as a process of repair and regeneration of the CNS (for review, see Reier and Houle, 1988). The hallmark of reactive astrocytosis is a prominent accumulation of GFAP (Eng, 1988).

Prion diseases, such as scrapie in animals and Creutzfeldt–Jakob disease in humans, are transmissible neurodegenerative disorders (spongiform encephalopathy) that cause typical reactive astrocytosis (Mackenzie, 1983; Weitgrefe et al., 1985; Manuelidis et al., 1987; Büeler et

al., 1993). Thus, it is important to determine whether GFAP has a role in the pathogenesis of prion diseases. S. B. Prusiner proposed the "protein only" hypothesis in which the prion, the infectious agent, is PrP^{Sc}, a modified form of the normal host protein PrP^{C} (Prusiner, 1982). Propagation of the prion is ascribed to the conversion of PrP^{C} into PrP^{Sc} under the influence of PrP^{Sc} (Prusiner, 1991). This hypothesis has been confirmed directly by experiments utilizing mice devoid of PrP^{C} generated by gene targeting (Büeler et al., 1993) and by experiments based on an in vitro cell-free system (Kocisko et al., 1994). However, it is not known whether any other molecule participates in either propagation of PrP^{Sc} or progression of the disease. Intriguing relationships between GFAP and infectious prions have been observed. The progression of prion disease causes a typical reactive astrocytosis along with increased GFAP expression (Weitgrefe et al., 1985; Manuelidis et al., 1987; Büeler et al., 1993). It has been suggested that high local concentrations of infectious Creutzfeldt–Jakob disease prion correlate with the level of *Gfap* mRNA expression in astrocytes, rather than with the severity of the neuronal degeneration (Manuelidis et al., 1987). Moreover, biochemical studies have revealed the specific binding of PrP^{Sc} to GFAP (Oesch et al., 1990). In this context, it is noteworthy that the conversion of PrP^{C} to PrP^{Sc} and the accumulation of PrP^{Sc} in astrocytes precede PrP^{Sc} conversion and accumulation in neurons in the course of the disease (Diedrich et al., 1991). These observations suggested a potential role for GFAP in the pathogenesis of prion diseases.

To address the function of GFAP in vivo, we used gene targeting to generate mutant mice in which the *Gfap* gene was disrupted by replacing it with the *lacZ* gene (Capecchi, 1989). Our specific goals were to determine whether GFAP is crucial for the development of the CNS and whether GFAP participates in the pathogenesis of scrapie-induced encephalopathy.

Results

The Mutation of the *Gfap* Locus

To generate a null mutation in the *Gfap* gene, we disrupted the first exon of the gene by gene targeting in embryonic stem (ES) cells. The targeting vector contains 5.5 kb of homologous sequences from the *Gfap* gene locus. The *pgk–neo* (McBurney et al., 1991) and *MC1-DT-A* (Yagi et al., 1990) gene cassettes were used as positive and negative selection markers, respectively (Figure 1A). The promoterless *lacZ*, a reporter gene, was inserted just downstream of the initiation codon of the *Gfap* gene in the sense orientation. Following homologous integration, this construct should express *lacZ* only at sites where the *Gfap* gene is normally transcriptionally active. The targeting vector was transfected into E14 ES cells (Hooper et al., 1987) by electroporation. Of the 232 ES clones analyzed, 25 were found to have the targeted mutation.

Cells from 5 clones were injected into C57BL/6J blastocysts; 3 clones gave rise to germline chimeras. Intercrosses between the heterozygotes ($Gfap^{+/-}$) gave rise to homozygotes ($Gfap^{-/-}$), $Gfap^{+/-}$, and wild types ($Gfap^{+/+}$) at the expected frequency of 1:2:1. An example of Southern analysis of tail DNAs from this cross is shown in Figure 1B.

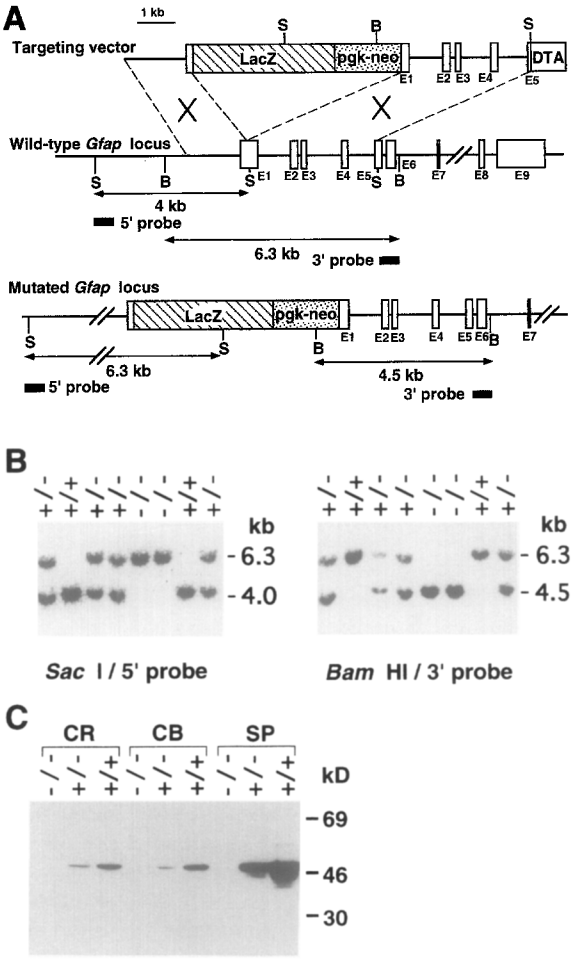

Figure 1. Targeted Disruption of the *Gfap* Gene with Insertion of the *lacZ* Gene

(A) Schematic representations of the targeting vector, wild-type *Gfap* locus, and mutant *Gfap* locus. The targeting vector used a neomycin resistance gene driven by the *pgk* promoter (*pgk–neo*) and a diphtheria toxin A-fragment gene (*DT-A*) driven by the *MC1* promoter as positive and negative selection markers, respectively. Exon structures (E1–E9) are shown with open boxes. The crosses indicate the hypothetical crossovers between the targeting construct and the *Gfap* locus. Homologous recombination results in replacement of the first exon of the *Gfap* gene with the *lacZ* gene and *pgk–neo*. The locations of the 5′ external probe (5′ probe) and the 3′ external probe (3′ probe) are shown. The 5′ probe hybridizes to a 4.0 kb SacI fragment from the wild-type *Gfap* locus and to a 6.3 kb SacI fragment from the mutated *Gfap* locus, and the 3′ probe hybridizes to a 6.3 kb BamHI fragment from the wild-type *Gfap* locus and to a 4.5 kb BamHI fragment from the mutated *Gfap* locus. S, SacI; B, BamHI.

(B) Southern blot analysis of progeny from a cross of F1 heterozygotes. Genomic DNA was extracted from tail, digested, and probed as described above. −/−, homozygotes; +/−, heterozygotes; +/+, wild type.

(C) Immunoblot analysis of tissue extracts (10 μg) using a monoclonal anti-GFAP antibody. The monoclonal antibody recognizes the 50 kDa GFAP in $Gfap^{+/+}$ and $Gfap^{+/-}$ mice but not in $Gfap^{-/-}$ mice. CR, cerebrum; CB, cerebellum; SP, spinal cord.

Mutant mice exhibit no striking behavioral changes and appear to have normal motor activity. The mutant mice

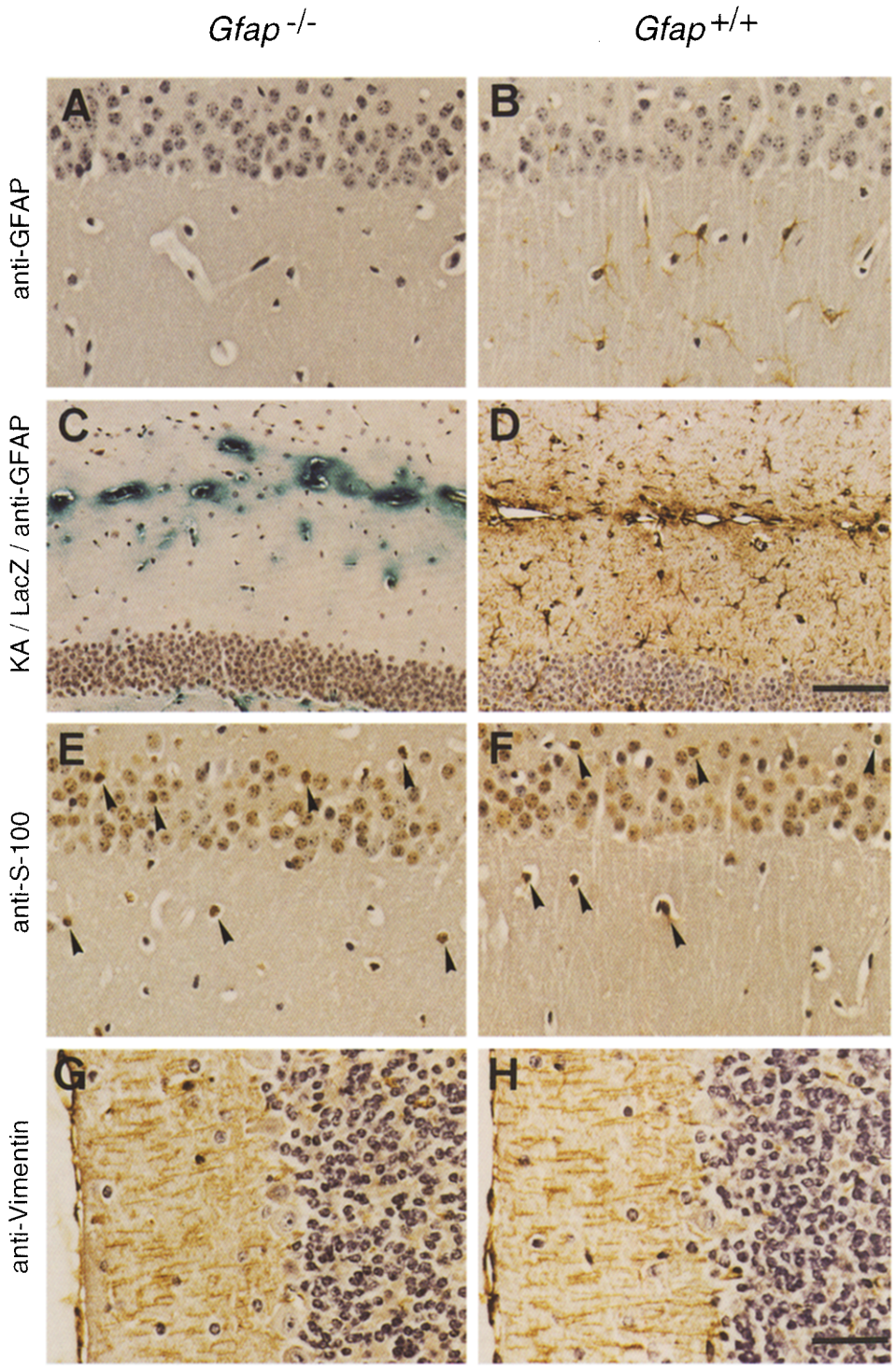

Figure 2. Histological Analysis of *Gfap*$^{-/-}$ and *Gfap*$^{+/+}$ Mice

Gfap$^{-/-}$ mutant (A, C, E, and G) and *Gfap*$^{+/+}$ (B, D, F, and H) mice. (A) and (B) show the hippocampal CA1 region in coronal sections labeled with an anti-GFAP monoclonal antibody; (C) and (D) show the expression of *lacZ* (C) or *Gfap* (D) in astrocytes induced by kainic acid treatment (KA). Kainic acid solubilized in phosphate-buffered saline (PBS) was administered intraperitoneally at the dose of 25 μg per gram of body weight. Brains from the treated mice were examined at 24 hr after the administration. Please note that the β-galactosidase-positive (C) and GFAP-positive (D) cells surround the blood vessels in the hippocampus. (E) and (F) show the CA1 region in coronal sections labeled for S-100. Astrocytes of *Gfap*$^{-/-}$ (E) and *Gfap*$^{+/+}$ (F) mice were intensively stained (indicated by arrowheads), whereas some neurons in the pyramidal cell layer were weakly stained. (G) and (H) illustrate the molecular and granule cell layers of cerebellum labeled for vimentin. Processes of Bergmann glia of both genotypes in the molecular layer show immunoreactivity. The sections were lightly counterstained with hematoxylin to indicate nuclei. Bars, 50 μm (A, B, and E–H), 100 μm (C and D).

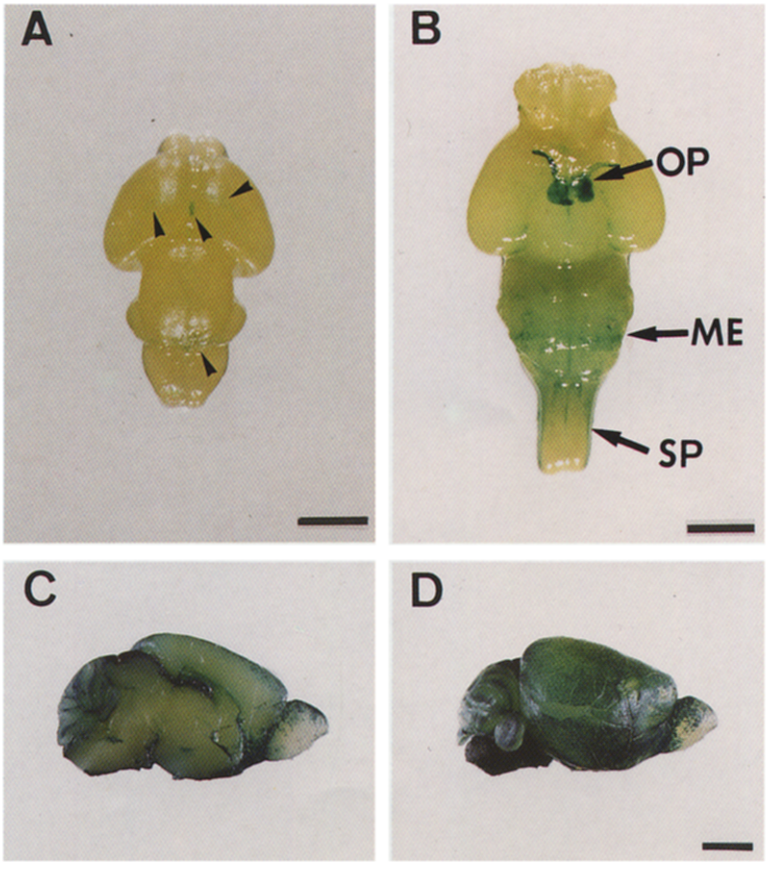

Figure 3. *lacZ* Expression during Development of *Gfap*$^{-/-}$ Mutant Mice

(A) Dorsal view of whole brain from a *Gfap*$^{-/-}$ mutant mouse at embryonic day (ED) 17.5. Weak *lacZ* expression is first detectable in the paraventricular regions of the lateral, third, and fourth ventricles (arrowheads).

(B) Ventral view of whole brain from a *Gfap*$^{-/-}$ mutant mouse at ED 18.5. *lacZ* expression is observed in the optic nerve (OP), medulla oblongata (ME), and spinal cord (SP).

(C and D) Medial (C) and lateral (D) views of a brain from a *Gfap*$^{-/-}$ mouse at postnatal day 15. *lacZ* is expressed in all brain regions and is especially strong in the pia mater, medulla oblongata, spinal cord, midbrain, corpus callosum, and cerebellar white matter. Bars, 2.5 mm.

grow up normally and are healthy at least up to the age that we have studied them (14 months). Both male and female *Gfap*$^{-/-}$ mice are fertile.

To confirm that the mutation introduced into the *Gfap* gene abolishes GFAP synthesis, littermates were subjected to Northern, immunoblot, and immunohistochemical analyses. Northern analysis detected no *Gfap* mRNA in the brain of *Gfap*$^{-/-}$ mice (data not shown). Immunoblot analysis of lysates from cerebrum, cerebellum, and spinal cord demonstrated the absence of GFAP in *Gfap*$^{-/-}$ mice and a reduced level of GFAP in *Gfap*$^{+/-}$ mice compared with *Gfap*$^{+/+}$ mice (Figure 1C). Representative data of immunohistochemical analysis are shown in Figure 2. Staining with anti-GFAP monoclonal antibody displayed the typical pattern of astrocytes in the brains of *Gfap*$^{+/+}$ mice (Figure 2B), whereas no staining was observed in *Gfap*$^{-/-}$ mice (Figure 2A). The data represented were obtained with a monoclonal antibody (GF12.24). Similar results were also obtained by using another monoclonal (6F2) and rabbit polyclonal antibodies in both immunoblot and immunohistochemical analyses. These results clearly demonstrate the complete lack of GFAP in the *Gfap*$^{-/-}$ mice.

Development of Astrocytes Devoid of GFAP

To analyze the development of astrocytes in the mutant mice lacking GFAP, we ontogenetically followed the expression of *lacZ* in the mutant mice. Several studies have shown that GFAP is first detectable during late embryonic development and that its immunoreactivity increases postnatally (Sapirstein, 1983; Weir et al., 1984). Whole-mount *lacZ* staining was performed on entire embryos from days 12.5 to 18.5 postcoitus. For postnatal 7-, 15-, and 20-day-old and 6-week-old mice, the brain and spinal cord were stained. As shown in Figure 3, *lacZ* expression was first detected in the paraventricular regions of the lateral, third, and fourth ventricles on embryonic day (ED) 17.5 (Figure 3A). At ED 18.5, the optic nerve, medulla oblongata, and spinal cord expressed *lacZ* (Figure 3B). After birth, *lacZ* was expressed in many other regions of the brain, with strong expression in the pia mater, optic nerve, corpus callosum, medulla oblongata, spinal cord, and cerebellar white matter (Figures 3C and 3D). β-Galactosidase activity declined in the brains of adult mice. The expression pattern correlated well with that of GFAP in *Gfap*$^{+/+}$ mice (data not shown), indicating the usefulness of β-galactosidase activity as a marker for GFAP-deficient astrocytes. However, β-galactosidase activity was slightly detectable by microscopy in cells scattered in most parenchymal regions. This seemed to be caused by diffusion of low amounts of β-galactosidase while preparing sections. When the mice were treated with kainic acid, β-galactosidase activity was strongly induced in mutant astrocytes, particularly in the hippocampus. Some cells expressing β-galactosidase surrounded the capillaries (Figure 2C), as normal astrocytes do (Figure 2D). Staining with an antibody against S-100, another marker protein for astrocytes

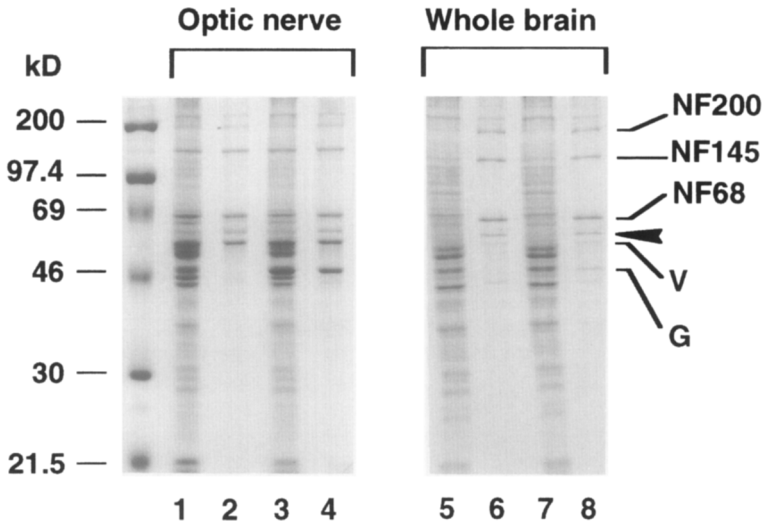

Figure 4. IF Proteins Expressed in the Optic Nerve and Brain of *Gfap*$^{-/-}$ Mice

SDS–polyacrylamide gel (10.5%) of total protein (lanes 1, 3, 5, and 7) and Triton-insoluble IF extracts (lanes 2, 4, 6, and 8) from the optic nerve and whole brain of *Gfap*$^{-/-}$ (lanes 1, 2, 5, and 6) and *Gfap*$^{+/+}$ (lanes 3, 4, 7, and 8) mice. The gel was stained with Coomassie blue. Positions of NF200, NF145, NF68, vimentin (V), and GFAP (G) are indicated on the right. The arrowhead indicates the 62 kDa protein. The size markers (in kilodaltons) are indicated on the left.

(Ludwin et al., 1976), also revealed that the distribution of the mutant astrocytes was similar to that of normal astrocytes (Figure 2E and 2F). Bergmann glia in the cerebellum, which express vimentin as well as GFAP in *Gfap*$^{+/+}$ mice, were also stained with anti-vimentin antibody in *Gfap*$^{-/-}$ mice. The shape and immunoreactivity of the processes of mutant Bergmann glia did not seem to be altered (Figures 2G and 2H). These results suggest that the development and localization of astrocytes are not significantly hampered by the lack of GFAP.

No Evidence for Compensatory Expression of Abnormal IF Proteins in Astrocytes of *Gfap*$^{-/-}$ Mice

To determine whether some other IF proteins are synthesized to take the place of GFAP in the mutant astrocytes, we analyzed cytoskeletal proteins, which are insoluble in nonionic solvent (Triton X-100), isolated from the optic nerves and whole brains of *Gfap*$^{-/-}$ mice by SDS–polyacrylamide gel electrophoresis (SDS–PAGE; Figure 4). The optic nerve is the tissue with the highest abundance of astrocytes. A Triton-insoluble fraction from optic nerve of *Gfap*$^{+/+}$ mice contained the neurofilament triplets (200 kDa NF, 145 kDa NF, and 68 kDa NF), 57 kDa vimentin, and 50 kDa GFAP. The identities of these proteins were confirmed by immunoblot analysis (data not shown). In addition to these proteins, a protein of 62 kDa was detected. The identity of this molecule is not yet clear; however, amino acid analysis indicated a similarity to the fourth neurofilament of 66 kDa identified in rat (Chiu et al., 1989; data not shown). This protein was hardly detectable in cultured astrocytes (data not shown), suggesting that it is specific to neurons. The fraction from *Gfap*$^{-/-}$ mice contained all of these proteins except GFAP. Several faint bands were observed in addition to molecules described above, but we did not observe quantitative differences in any proteins between mutant and wild-type fractions analyzed. Similar results were obtained with whole-brain extracts (Figure 4).

Consistently, anti-cytokeratins and anti-desmin antibodies showed no immunoreactivity in astrocytes of mutant mice. Together, these results render it unlikely that the lack of GFAP leads to the compensatory expression of alternative IF protein(s) in astrocytes of *Gfap*$^{-/-}$ mice.

Normal Development of CNS in *Gfap*$^{-/-}$ Mice

Several lines of evidence from in vitro studies have suggested direct interactions between neurons and astrocytes. Furthermore, both cell types develop from a common progenitor. Therefore, the mutation of *Gfap* may alter the development of neurons. However, we found no apparent histological differences in brain architecture between *Gfap*$^{-/-}$ mutant and wild-type mice. Immunohistology with antibodies against actin, α-tubulin, neurofilaments, microtubule-associated protein 1 (MAP1), neural cell adhesion molecule (N-CAM), and CNPase also failed to reveal any detectable abnormality (data not shown). Cell numbers in tempolateral cortex and thalamus counted at different ages (15-day-old and 6-, 16-, and 36-week-old) were similar in *Gfap*$^{-/-}$ and *Gfap*$^{+/+}$ mice (data not shown).

To evaluate the function of BBB, peroxidase trace experiments (Reese and Karnovsky, 1967) were performed in *Gfap*$^{-/-}$ mutant and *Gfap*$^{+/+}$ mice . Horseradish peroxidase or microperoxidase was injected intravenously, and the brains were subsequently fixed and sliced. Then, the extravasation of peroxidase was detected by diaminobenzidine reaction. No leakage of peroxidase was observed with light or electron microscopic analysis in the brains of *Gfap*$^{-/-}$ mutant mice (data not shown), except for the regions in which leakage is commonly observed in the normal brain, such as the paraventricular region of the third ventricle. This result suggests that deficiency of GFAP in astrocytes does not interfere with the establishment and maintenance of the BBB.

From these results, it appears that the *Gfap* gene is not

Table 1. Summary of Scrapie Infection Experiments in *Gfap*$^{-/-}$, *Gfap*$^{+/-}$, and *Gfap*$^{+/+}$ Mice

Genotype	Susceptibility to Scrapie Prion			Prion Titers in Brains of Inoculated Mice (Log LD_{50}/g)		
	No. of Mice Inoculated[a]	Appearance of Symptom (days)	Survival Days (mean ± SD)	2 wks	12 wks	20 wks
Gfap$^{+/+}$	14	143–153	175 ± 2	<3.0[d]	7.35	7.85
	(10)	(–)[b]	(–)[c]	ND	ND	ND
Gfap$^{+/-}$	21	143–153	172 ± 3	<3.0	7.39	7.89
	(12)	(–)	(–)	ND	ND	ND
Gfap$^{-/-}$	15	143–153	175 ± 2	<3.0[e]	6.98	7.83
	(10)	(–)	(–)	ND	ND	ND
ICR/Slc	3	143	176 ± 2	ND	ND	ND

[a] Numbers of mice inoculated with a dose ($10^{2.8}$ LD_{50} per animal) of mouse-adapted Obihiro strain of scrapie prion (Shinagawa et al., 1985). Parentheses indicate the number of mice inoculated with extract from brains of normal mice as a mock inoculation.
[b] Minus sign indicates no appearance of disease during the observation period.
[c] Minus sign indicates that all mice survived during the observation period. The titers in brains recovered at 2, 12, and 20 weeks after inoculation (wks) were determined according to the procedure described by Prusiner et al. (1982).
[d] One of 5 mice inoculated developed symptoms at 290 days.
[e] One of 5 mice inoculated developed symptoms at 220 days. ND, not determined.

essential for the development and basic functions of the murine CNS.

Inoculation of Scrapie Prion (PrP^{Sc}) in *Gfap*$^{-/-}$ Mutant Mice

Gfap$^{-/-}$, *Gfap*$^{+/-}$, and *Gfap*$^{+/+}$ mice (7- to 8-week-old) were inoculated intracerebrally with a dose ($10^{2.8}$ LD_{50} per animal) of mouse-adapted Obihiro strain of scrapie prion (PrP^{Sc}; Shinagawa et al., 1985). The genetic background of *Gfap*$^{-/-}$, *Gfap*$^{+/-}$, and *Gfap*$^{+/+}$ mice is derived from 129/Ola and C57BL/6J strains. The 129 and C57BL/6 strains have the haplotype *a* of prion protein gene (*Prn-p*^{a}) alleles, which causes a short scrapie incubation period (Carlson et al., 1988). As a control, ICR/Slc mice, a strain used for the determination of prion titer, were inoculated with PrP^{Sc}. The mice were sacrificed at 2, 12, 20, and 23 weeks after inoculation for histological and biochemical analyses. As a control, mice mock-infected with lysates from normal mouse brains were also examined in the same manner (Table 1).

ICR/Slc mice first showed typical neurological symptoms at 143 days of inoculation and died at 176 ± 2 days. Similarly, *Gfap*$^{-/-}$, *Gfap*$^{+/-}$, and *Gfap*$^{+/+}$ mice first showed the neurological symptoms at 143–153 days and died at 175 ± 2, 172 ± 3, and 173 ± 4 days, respectively (Table 1). No striking differences were observed in the neurological symptoms displayed by these three different genotypes.

For the detection of scrapie prion (PrP^{Sc}), extracts were prepared from brains of infected mice, and immunoblotting was performed using polyclonal anti-prion protein (PrP) antiserum obtained by immunization of a rabbit against a synthetic peptide corresponding to amino acids 213–226 of mouse PrP (Yokoyama et al., unpublished data). The proteinase K–resistant PrP^{Sc} was detected in all mouse brain extracts 20 weeks after inoculation (data not shown). For the immunohistochemical detection of PrP amyloid plaques, tissue sections were stained with the above antibody. PrP amyloid plaques were found in various regions of the brain, such as the cerebral cortex, corpus callosum, hippocampus, and thalamus, both in scrapie-infected *Gfap*$^{-/-}$ and *Gfap*$^{+/+}$ mice (Figures 5A and 5B). No plaques were observed in mock-infected brains.

At 2, 12, and 20 weeks after inoculation, brains from 2–4 mice were sampled and used for the infectivity titration assay. The samples were homogenized in phosphate-buffered saline (PBS), and a pool of the extracts was inoculated intracerebrally into 5–7 ICR/Slc mice per group. Significant propagation of infectious units was detected in *Gfap*$^{-/-}$ mice as well as *Gfap*$^{+/-}$ and *Gfap*$^{+/+}$ mice by 12 weeks of inoculation (Table 1). We did not observe significant differences in infectivities from the three genotypes.

These data reveal that GFAP-deficient mice are as susceptible to scrapie prion as normal mice, and that GFAP molecules do not significantly affect the propagation of PrP^{Sc} in the brain of mice.

Astrocytic Responses in Scrapie-Infected *Gfap*$^{-/-}$ Mutant Mice

To evaluate the scrapie-induced neuropathology, brains of scrapie-infected and mock-infected *Gfap*$^{-/-}$ and *Gfap*$^{+/+}$ mice were analyzed histologically. Both scrapie-infected *Gfap*$^{-/-}$ and *Gfap*$^{+/+}$ mice showed vacuolative changes (spongiform degeneration typical of scrapie encephalopathy) in the cortex (Figures 5E and 5F), hippocampus (Figures 5I and 5J), and thalamus (data not shown) at 20 and 23 weeks after infection. Scrapie-infected *Gfap*$^{+/+}$ mice showed remarkable reactive astrocytosis as detected by immunostaining with an anti-GFAP antibody (Figures 5F and 5J). Since the same staining gave rise to no signal in *Gfap*$^{-/-}$ mice (Figures 5E and 5I), the reactive response of mutant astrocytes in *Gfap*$^{-/-}$ mice was evaluated by *lacZ* staining. Figure 6 shows β-galactosidase activities in the brains of scrapie-infected and mock-infected *Gfap*$^{-/-}$ mice at 2, 12, 20, and 23 weeks after inoculation. A significant induction of β-galactosidase activity was first observed at 12 weeks after infection (in hippocampus and thalamus; Figure 6, arrows), and the activity increased dramatically by 23 weeks after infection (Figures 5E and 5I; Figure 6).

Vimentin is known to be expressed in reactive astrocytes

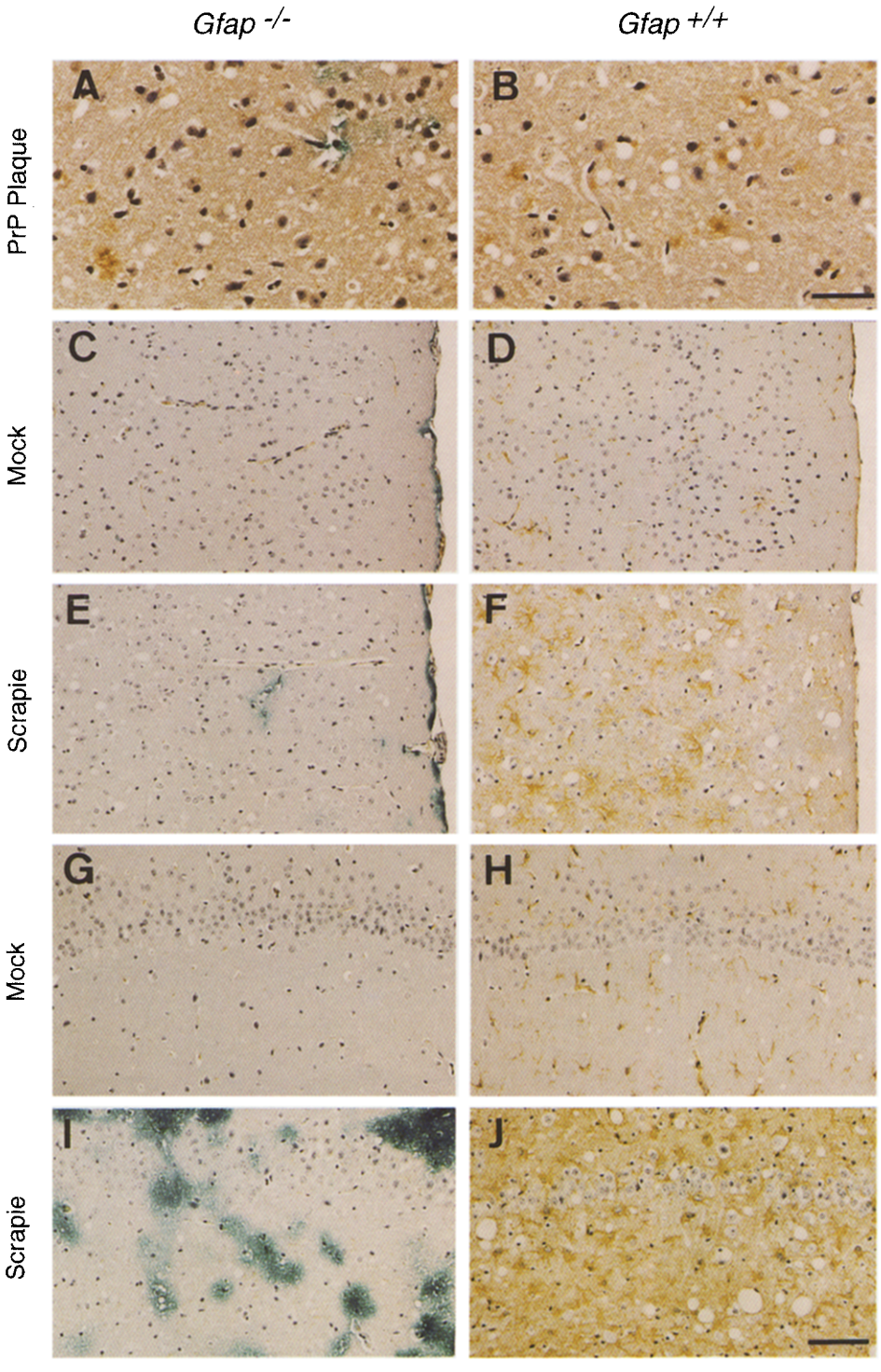

Figure 5. Histopathology of Brains from *Gfap*$^{-/-}$ and *Gfap*$^{+/+}$ Mice Infected with Scrapie

Gfap$^{-/-}$ mutant (A, C, E, G, and I) and *Gfap*$^{+/+}$ (B, D, F, H, and J) mice at 23 weeks after inoculation. PrP amyloid plaques in the cerebral cortex of *Gfap*$^{-/-}$ (A) and *Gfap*$^{+/+}$ (B). Peroxidase immunohistochemistry was performed with an antiserum obtained by immunization of rabbit with the synthetic peptide that corresponds to amino acids 213–226 of mouse PrP. Double staining for GFAP and β-galactosidase was performed on the tempolateral cortex of cerebrum (C–F) and CA1 region of hippocampus (G–J). The vacuolative changes were observed in the cortex and hippocampus of scrapie-infected *Gfap*$^{-/-}$ and *Gfap*$^{+/+}$ mice (E, F, I, and J). In mock-infected *Gfap*$^{+/+}$ mice, scattered astrocytes with slender GFAP-positive processes are observed (D and H), whereas numerous reactive astrocytes with hypertrophic cytoplasm and strongly GFAP-positive processes were observed in scrapie-infected *Gfap*$^{+/+}$ mice (F and J). In *Gfap*$^{-/-}$ mice, an increased expression of *lacZ* in the cortex and hippocampus occurs in scrapie-infected (E and I) brain. No GFAP immunoreactivity was detected in mock-infected (C and G) or scrapie-infected (E and I) brains from mutant mice. The sections were lightly counterstained with hematoxylin. Bars, 50 μm (A and B), 100 μm (C–H).

Figure 6. *lacZ* Expression in Brains from Scrapie-Infected *Gfap*$^{-/-}$ Mice

Coronal brain sections through the hippocampal and thalamic regions. Mock-infected (Mock) and scrapie-infected (Scrapie) brains at 2, 12, 20, and 23 weeks after inoculation are aligned in the left and right columns, respectively. Increased *lacZ* expression was first evident in the hippocampus and thalamus 12 weeks after infection (indicated by arrows). By 23 weeks after scrapie infection, the β-galactosidase activity had increased dramatically in a wide area of the brain regions.

(Dahl et al., 1981; Pixley and de Vellis, 1984; Schiffer et al., 1986; Petito et al., 1990), in contrast to most astrocytes under physiological conditions. Therefore, we analyzed the astrocytic reactivity in scrapie-infected *Gfap*$^{-/-}$ mice by vimentin immunocytochemistry. Moderate vimentin immunoreactivity was observed in the cytoplasm of reactive astrocytes of scrapie-infected *Gfap*$^{+/+}$ mice (Figure 7A). Immunoreactivity against S-100 protein, a marker for astrocytes, was also detected in reactive astrocytes of scrapie-infected *Gfap*$^{+/+}$ mice (Figure 7C). In *Gfap*$^{-/-}$ mice, β-galactosidase-positive mutant astrocytes were colabeled with anti-vimentin and anti-S-100 antibodies (Figures 7E and 7F), indicating their astrocytic identity. However, the immunostaining of vimentin and S-100 protein in *Gfap*$^{-/-}$ astrocytes was slightly different from that of *Gfap*$^{+/+}$ reactive astrocytes (compare Figures 7A and 7B for vimentin and Figures 7C and 7D for S-100). Vimentin signals are filamentous and fill the cytoplasms of *Gfap*$^{+/+}$ reactive astrocytes (Figure 7A). In contrast, vimentin signals in mutant astrocytes tend to be granular and scarce around the nuclei (Figure 7B). S-100 protein is normally localized to the nuclei and cytoplasm of reactive astrocytes (Figure 7C). The anti-S-100 antibody strongly stained the nuclei of the astrocytes of *Gfap*$^{-/-}$ (Figure 7D) as well as *Gfap*$^{+/+}$ mice. However, similar to anti-vimentin staining, S-100 signals are scarce in the cytoplasm of mutant astrocytes, particularly around the nuclei (Figure 7D).

In agreement with the immunohistochemistry, immunoblot analysis clearly showed an increase of GFAP and vimentin in the brains of scrapie-infected *Gfap*$^{+/+}$ mice 20 weeks after inoculation. In the brains of scrapie-infected *Gfap*$^{-/-}$ mice, increased vimentin expression was also detected by immunoblotting (data not shown).

These results show that scrapie-specific neuropathology is induced in the brain of *Gfap*$^{-/-}$mice. Furthermore, they suggest that GFAP is not essential for the induction of reactive astrocytosis.

Discussion

In the present study, we disrupted the *Gfap* gene in mice by replacing a short fragment of the first exon with the *lacZ* gene using ES cell technology. GFAP expression in astrocytes is thought to be important for the morphogenesis and structural support of the CNS. However, mutant mice devoid of GFAP exhibit no obvious defects in development and tissue architecture in the CNS. Astrocytes lacking GFAP have a normal distribution, and the mutation did not result in any detectable deficiency of neuronal development. Additionally, the mutant astrocytes extend their processes to capillaries as normal cells do. Electron microscopic analysis and peroxidase permeability tests showed that the BBB is structurally normal in *Gfap*$^{-/-}$ mutant mice (data not shown).

The lack of any apparent defects in the mutant mice suggests that GFAP does not have an essential role in the development of astrocytes. Astrocytes are known to be heterogeneous in cell shape and probably in function. Some astrocytes do not contain detectable amounts of GFAP in vivo. Given the fact that the null mutation in the *Gfap* gene does not induce compensatory expression of alternative IF proteins, the data may suggest that no IF proteins are required for the physiology of some types of astrocytes. Very recently, vimentin knockout mice were generated (Colucci-Guyon et al., 1994). The mice devoid of vimentin have not shown any apparent defects. As in the case of GFAP, there was no evidence for the compensatory expression of alternative IF proteins in the vimentin-deficient mice, and a complete lack of any IF networks in vivo was observed in the lens fibers from these mutant mice.

Even though the above interpretation is true for some astrocytes, it is also possible that some other molecule(s) functionally compensate for the lack of GFAP. In the course of astrocyte development, a transition in expression of IF protein genes has been observed (Hockfield and McKay, 1985; Lendahl et al., 1990; Fliegner and Liem, 1991; Liem, 1993). Proliferating neuroepithelial stem cells, which can differentiate into neurons and glia, express vi-

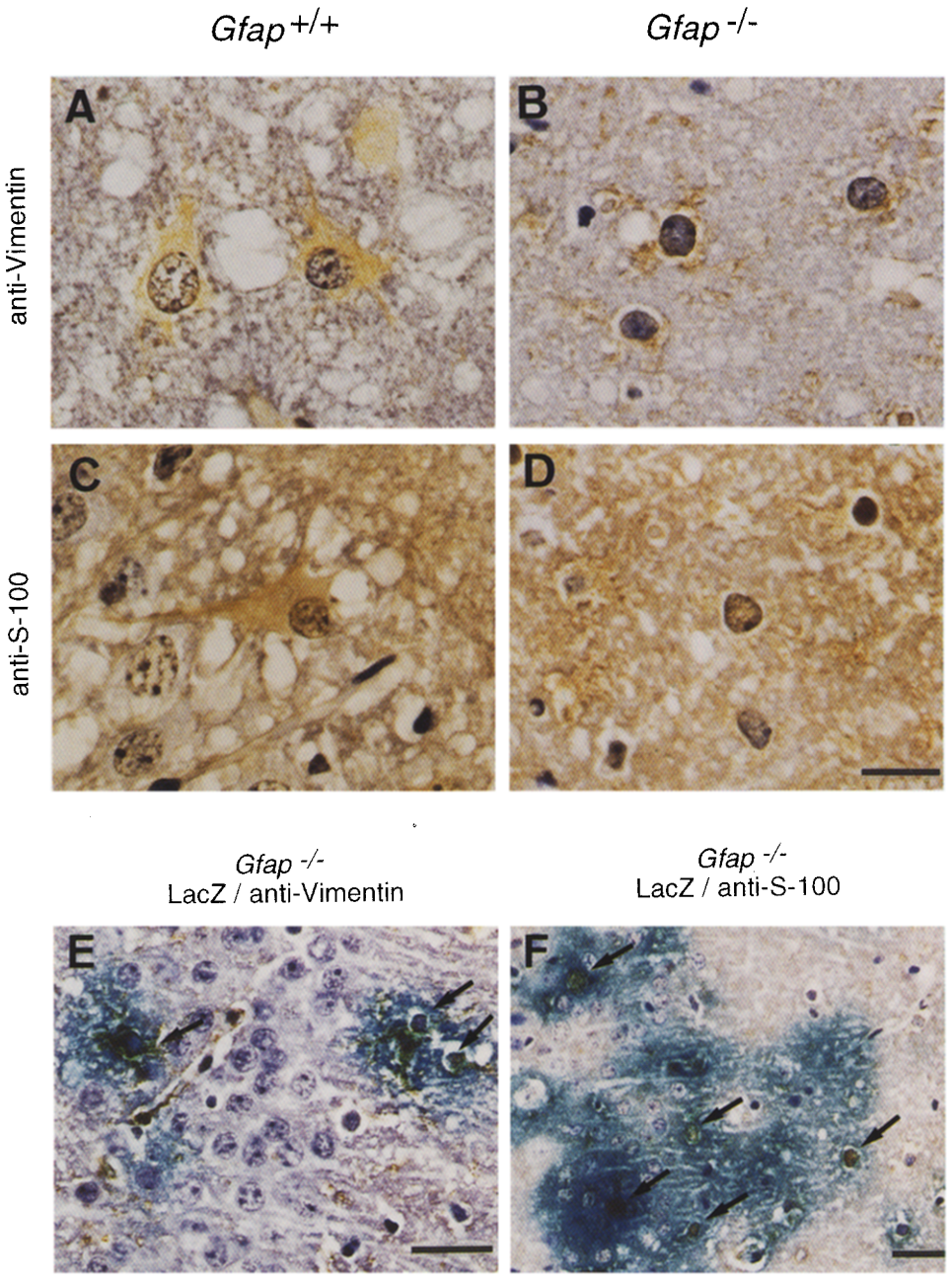

Figure 7. Astrocytic Changes Shown by Vimentin and S-100 Staining in the Brains of *Gfap*$^{-/-}$ and *Gfap*$^{+/+}$ Mice Infected with Scrapie

Mice brain sections at 23 weeks after scrapie inoculation. Vimentin immunoreactivity is shown in the cytoplasm (A), whereas S-100 immunoreactivity is located in both the cytoplasm and the nucleus (C) of reactive astrocytes in *Gfap*$^{+/+}$ mice. Please note in *Gfap*$^{-/-}$ mice, vimentin immunoreactivity is granular (B), and S-100 immunoreactivity is strong in the nucleus but not in the cytoplasm (D). In *Gfap*$^{-/-}$ mice, *lacZ*-expressing cells show vimentin (E) and S-100 (F) immunoreactivities (arrows). The sections were lightly counterstained with hematoxylin. Bars, 20 μm (A–D), 25 μm (E and F).

mentin and nestin (Frederiksen and McKay, 1988; Lendahl et al., 1990). Radial glial cells that differentiate into CNS astrocytes (Schmechel and Rakic, 1979) express both vimentin and nestin (Hockfield and McKay, 1985). GFAP-negative and vimentin-positive radial glia of rat disappear at an early postnatal stage, whereas the expression of GFAP in mature astrocytes dramatically increases between birth and postnatal day 20 (Pixley and de Vellis, 1984). Nestin is absent in astrocytes from adult brain, whereas vimentin is constitutively expressed in some mature astrocytes, such as the astrocytes in the optic nerve, Bergmann glial cells in cerebellum, and white matter astrocytes in the adult brain (Schnitzer et al., 1981; Yokoyama et al., 1981; Pixley et al., 1984; Pixley and de Vellis, 1984). Furthermore, vimentin is induced in reactive astrocytes following neuronal damage (Dahl et al., 1981; Pixley

and de Vellis, 1984; Schiffer et al., 1986; Petito et al., 1990) and in in vitro–cultured astrocytes, suggesting that the *Vim* locus is not completely silent in mature astrocytes, in which vimentin is hardly detectable in vivo. Therefore, vimentin may in part compensate for the lack of GFAP. Very small amounts of vimentin could be sufficient for the putative functional compensation. The hypothesis discussed above should be tested by generating double knockout mice for GFAP and vimentin.

Since the IF proteins comprise a very large gene family, more unidentified IF proteins may be involved in the putative compensation. Indeed, a monoclonal antibody (34C9) that reacts with an epitope of human epidermal keratin has been demonstrated to bind to a cytoskeletal fiber structure closely associated with GFAP in a subclass of astrocytes of the adult hamster brain and in astrocytes in fetal mouse brain cultures (Franko et al., 1987). In immunoblot analysis, the 34C9 monoclonal antibody was shown to recognize a 65 kDa protein (p65) and not to recognize GFAP. This observation suggests that epidermal keratins share an epitope not only among themselves but also with a keratin in neuronal tissue. The p65 might be a restricted IF protein that copolymerizes with GFAP. Alternatively, it could be an IF-associated protein. This protein is another candidate molecule that may compensate for the lack of GFAP.

GFAP accumulation in reactive astrocytes has been observed in scrapie-infected brain (Mackenzie, 1983; Wietgrefe et al., 1985; Kretzschmar et al., 1986; Büeler et al., 1993) and human brain with Creutzfeldt–Jakob disease (Hirano et al., 1972). Interestingly, previous biochemical studies by Oesch et al. (1990) showed a high affinity of PrP^{Sc} or its cellular form, PrP^{C}, to GFAP. It was therefore important to determine whether GFAP has a role in the pathogenesis of prion diseases. In this study, *Gfap*$^{-/-}$ mice infected with PrP^{Sc} showed the same scrapie-specific neuropathology and the same disease time course as did scrapie-infected *Gfap*$^{+/+}$ mice. Our results revealed that *Gfap*$^{-/-}$ mice have a normal susceptibility to scrapie infection and are unaffected in the propagation of PrP^{Sc}. These results indicate that GFAP is not crucial for scrapie-induced neuropathogenesis. However, we cannot exclude the possibility that the interaction between GFAP and PrP^{C} is physiologically required for astrocytic functions, and in turn for some neuronal activities. PrP^{C} mRNA and protein, abundantly expressed in neurons, have been detected in many cell types, including astrocytes (Kretzschmar et al., 1986; DeArmond et al., 1987; Brown et al., 1990; Cashman et al., 1990). Interestingly, it has been shown recently that hippocampal slices from PrP null mutant mice have weakened γ-aminobutyric acid type A receptor–mediated fast inhibition and impaired long-term potentiation (Collinge et al., 1994). The remaining issue could be tested by analyzing the cumulative effects on these activities in double knockout mice for GFAP and PrP.

The scrapie prion is known to be a strong inducer of reactive astrocytes. The progression of the prion diseases results in typical reactive astrocytosis. The reactive astrocytes are histologically characterized by cytoplasmic hypertrophy associated with profusion of long and thick processes filled with GFAP, and often by enlarged and irregularly outlined nuclei. Astrocytes devoid of GFAP in *Gfap*$^{-/-}$ mutant mice showed increased *lacZ* expression along with the progression of disease, correlating with accumulation of GFAP in wild-type mice. Increased expression of vimentin was also detected in the astrocytes of mutant as well as wild-type mice by immunoblot and immunocytochemical analysis. These results suggest that the astrocytes devoid of GFAP are able to be transformed to a reactive state, and that the β-galactosidase activity in the mutant astrocytes is a useful marker for the reactive state. The β-galactosidase activity may reflect the *Gfap* gene transcriptional activity better than the level of GFAP protein itself, whose stability could be altered by polymerization. Therefore, the mutant mice generated here may provide a useful tool to analyze the induction mechanisms for reactive responses of astrocytes.

The mutant astrocytes from scrapie-infected mice showed subtle differences from wild-type reactive astrocytes in stainability with anti-S-100 and anti-vimentin antibodies. The mutant astrocytes did not seem to have the normal cytoplasmic localization of these molecules. S-100 protein, which is a calcium-binding, glial-specific protein, is known to bind to GFAP and prohibit its polymerization in vitro (Bianchi et al., 1993). Vimentin is known to copolymerize with GFAP (Quinlan and Franke, 1983; Wang et al., 1984). Therefore, it is not surprising that the lack of GFAP might have altered the subcellular localization and/or polymerization of these molecules. The consequences of these observations are not yet known. However, if the subcellular distribution of these and other molecules were altered in astrocytes under normal physiological conditions, the mutation might alter the physiological functions specific for astrocytes. Additional electrophysiological and biochemical studies are required to analyze this issue further.

Experimental Procedures

Construction of the Targeting Vector

A genomic DNA clone of mouse GFAP was isolated from a 129/Sv genomic library by screening with a mouse DNA fragment previously amplified by polymerase chain reaction. The fragments used were a 2.0 kb SalI fragment of the promoter region, a 3.5 kb SacI fragment from exon 1 to intron 1, a 3.7 kb HindIII–BamHI *lacZ* gene fragment prepared from pCH110 (Pharmacia), a 1.8 kb *pgk–neo* gene cassette derived from pKJ1 (McBurney et al., 1991; a gift from Michael A. Rudnicki), and a 1.0 kb XhoI–SalI diphtheria toxin A-fragment (DT-A) gene cassette derived from pMC1DT-A (Yagi et al., 1990; a gift of Shinichi Aizawa). The resulting construct could transcribe the *lacZ* gene from the GFAP promoter and abolish the transcription of the *Gfap* gene.

Targeting Experiments

The ES cell line used was E14 (Hooper et al., 1987). Cell culture and the targeting experiment were carried out as described previously (Itohara et al., 1993). In brief, 5×10^7 ES cells were electroporated with a Bio-Rad Gene Pulser (800 V and 3 mF in a 0.4 cm electrode distance) using 30 μg of DNA. Prior to electroporation, the targeting vector was linearized by digestion with NotI. The electroporated cells were plated in ten 10 cm dishes coated with mitotically inactivated embryonic fibroblasts derived from the *TCR δ* gene knockout mice (Itohara et al., 1993). G418 was added 24 hr after electroporation, and colonies were picked at day 7 of selection into wells of 96-well plates. The cells were cultured and passaged into 24-well plates, and half of the cells were stored in liquid nitrogen until the completion of screen-

ing. The other half of the cells were screened by digestion with SacI or BamHI and hybridization with a 5′ external probe (5′ probe; a 0.5 kb SacI–BalI fragment) or a 3′ external probe (3′ probe; a 0.4 kb HindIII–BamHI fragment). Southern blots were analyzed using a Fujix Bio-Image Analyzer BAS2000.

Generation of Chimeric Mice and Screening of Mutant Mice

Chimeras were generated as described (Bradley, 1987). ES cells (15–20) were microinjected into C57BL/6J blastocysts at 3.5 days post-coitum. After injection, the embryos were transferred into the uteri of pseudopregnant ICR mice. Mice heterozygous for the mutation (*Gfap*$^{+/-}$) were obtained by crossing the chimeras to C57BL/6J mice. The heterozygotes (*Gfap*$^{+/-}$) were further intercrossed to obtain mutation homozygotes (*Gfap*$^{-/-}$). The genotypes of the mice were determined by Southern blot analysis of DNA prepared from tails, as mentioned above.

Histological Analysis

For *lacZ* staining of brain and spinal cord, mice were anesthetized with Nembutal, and brains were fixed by immersion or intracardiac perfusion with fixative solution containing 2% formaldehyde, 2 mM $MgCl_2$, and 1.25 mM EGTA in 0.1 M PIPES (pH 6.9), followed by perfusion with PBS at 4°C. Samples were washed three times in 50 mM phosphate buffer (pH 7.3) and stained at 37°C overnight in a solution containing 5 mM $K_3Fe(CN)_6$, 5 mM $K_4Fe(CN)_6$, 2 mM $MgCl_2$, 0.02% Nonidet P-40, 0.01% sodium deoxycholate, and 1 mg/ml X-gal (5-bromo-4-chloro-3-indoyl-β-D-galactopyranoside) in the phosphate buffer.

For paraffin sections, fresh samples were fixed with neutral buffered formalin or ethanol, and *lacZ*-stained samples were postfixed in 2% formaldehyde in the phosphate buffer, dehydrated, and embedded in paraffin. Sections (4 μm) were used for hematoxylin–eosin and immunohistochemical staining.

The immunohistochemical detection was performed with an avidin–biotin–peroxidase technique using the Vectastain ABC kit (Vector Lab.) following the manufacturer's instructions. Anti-GFAP (GF 12.24), anti-vimentin (VIM 3B4), and anti-cytokeratin 8 (Ks 8.7) and 18 (Ks 18.4) monoclonal antibodies were purchased from Progen Biotechnic. Another anti-GFAP monoclonal (6F2) and rabbit anti-GFAP polyclonal antibodies were purchased from Monosan. Monoclonal antibodies to neurofilament 68 kDa, 145 kDa, and 200 kDa subunits were purchased from Transformation Research Inc. Anti-S-100 protein (15E2) and anti-actin monoclonal antibodies were purchased from Chemicon International Inc. Anti-vimentin (V9), anti-desmin (DE-U-10), anti-α-tubulin (DM 1A), anti-CNPase (11–5B), anti-N-CAM (NCAM-OB11), and anti-MAP1 (HM-1) monoclonal antibodies were purchased from Sigma.

Biochemical Analysis

Mouse brain extracts were analyzed by SDS–PAGE (Laemmli, 1970) and immunoblotting. The cerebrum, cerebellum, spinal cord, and optic nerves were homogenized in lysis buffer (50 mM sodium phosphate (pH 7.3), 2 mM EDTA, 2 mM EGTA, 0.5 mM TPCK, 0.8 mM phenylmethylsulfonyl fluoride [PMSF]), and an equal volume of 2× SDS-sample buffer (0.25 M Tris–HCl [pH 6.8], 2% SDS, 50% glycerol, 10% 2-mercaptoethanol) was added. Protein (10 μg) was electrophoresed on 10.5% polyacrylamide gels and blotted on an Immobilon-P membrane (Milipore). After blocking the membrane with 5% skim milk in Tris-buffered saline, the blots were immersed sequentially in mouse monoclonal primary antibodies (1:50 to 1:300) and peroxidase-conjugated rat anti–mouse IgG (1:5000; Zymed Laboratories Inc.) and developed in ECL Western blotting detection reagent (Amersham).

Triton-insoluble cytoskeletal proteins from optic nerve and brain were prepared as described by Pruss et al. (1981). The tissues were homogenized with ice-cold PBS consisting of 171 mM NaCl, 6 mM sodium phosphate (pH 7.4), 3 mM KCl, 2 mM EDTA, 2 mM EGTA, and 1 mM PMSF. This homogenate was centrifuged at 8000 × g for 10 min at 4 °C, and the pellet was extracted with an extraction buffer containing 171 mM NaCl, 6 mM sodium phosphate (pH 7.4), 600 mM KCl, 0.5% (w/v) Triton X-100, 1 mM EDTA, 1 mM EGTA, and 1 mM PMSF. This homogenate was centrifuged again at 8000 × g for 10 min at 4°C, and the pellet was re-extracted twice with the extraction buffer. The final Triton-insoluble pellet was washed four times with ice-cold washing buffer containing 171 mM NaCl, 6 mM sodium phosphate (pH 7.4), and 3 mM KCl.

Inoculation of Scrapie Prion

The Obihiro strain of scrapie prion (PrP^{Sc}), which has been passaged in ICR/Slc mice more than ten times (Shinagawa et al. 1985) was prepared from infected brains homogenized in PBS and intracerebrally inoculated ($10^{2.8}$ LD_{50}/animal) into 7- to 8-week-old *Gfap*$^{-/-}$, *Gfap*$^{+/-}$, and *Gfap*$^{+/+}$ mice. Normal brain homogenates (10%) were used for mock infection experiments. As a further control, ICR/Slc mice were inoculated with PrP^{Sc}. Mice were observed daily for the appearance of scrapie-associated symptoms, i.e., ataxia, ruffled hair, disorientation, and depression. Mice were examined histologically and biochemically at 2, 12, 20, and 23 weeks after inoculation.

For biochemical analysis, PrP^{Sc} was purified by the procedure of Hilmert and Diringer (1984) with minor modifications to use a bench top ultracentrifuge Beckman Optima TL. Briefly, brain samples were homogenized with 10 mM Tris buffer (pH 7.4) containing 10% sarcosyl and then centrifuged at 22,000 × g for 10 min. The supernatant was centrifuged at 540,000 × g for 30 min. The resulting pellet was sonicated in Tris buffer containing 1% sarcosyl and 10% NaCl and centrifuged again at 540,000 × g for 30 min. The pellet was treated with proteinase K (2 μg per gram of brain equivalent) at 37°C for 60 min and centrifuged three times at 22,000 × g for 10 min. The final pellet was subjected to SDS–PAGE (15% polyacrylamide gel). Immunoblotting was performed using polyclonal anti-prion protein (PrP) antiserum obtained by immunization of rabbit against the synthetic peptide that corresponds to the sequence at amino acids 213–226 (CVTQYQKES-QAYYD) of mouse PrP (Yokoyama et al., unpublished data).

For the immunohistochemical detection of PrP amyloid plaques, tissue sections were deparaffinized, followed by dehydration and autoclaving (121°C, 10 min) in distilled water. Sections were reacted with the above-mentioned primary antibody at a 1:350 dilution and a secondary anti–rabbit IgG using the Vectastain ABC kit.

The infectivity in the brains of infected mice was determined according to a published procedure (Prusiner et al., 1982). Brain samples were homogenized in PBS at 10% or 1% (w/v). Mice were inoculated intracerebrally with 20 μl of the homogenates. The procedure is based on the correlation between the titer and the incubation period. One of us (T. Y.) has confirmed the reliability of the assay by separate experiments.

Acknowledgments

All correspondence should be addressed to S. I. We thank Yasuyuki Inoue for his excellent technical assistance and Kenkichi Imamura, Syouei Okamoto, Mitsuhiko Hoshimura, and Hiroyuki Sato for their help maintaining the mouse colony. We thank David Gerber and Alcino Silva for reviewing the manuscript. We thank Charles Babinet for showing us their preprints. We thank Susumu Tonegawa for his invaluable help, continuous encouragement, and critical reading. We thank Noboru Yuasa for his encouragement. We thank Miho Rokutanda for secretarial assistance. We thank Martin Hooper, Michael Rudnicki, and Shinichi Aizawa for providing the E14 cell line, *pgk–neo*, and pMC1-DT-A, respectively. This work was supported by grants from the Ministry of Education, Science, and Culture, the Science and Technology Agency of Japan, and the Shionogi Institute for Medical Science.

The costs of publication of this article were defrayed in part by the payment of page charges. This article must therefore be hereby marked *"advertisement"* in accordance with 18 USC Section 1734 solely to indicate this fact.

Received September 9, 1994; revised October 17, 1994.

References

Arthur, F. E., Shivers, R. R., and Bowman, P. D. (1987). Astrocyte-mediated induction of tight junctions in brain capillary endothelium: an efficient *in vitro* model. Dev. Brain Res. *36*, 155–159.

Baribault, H., Price, J., Miyai, K., and Oshima, R. G. (1993). Mid-gestational lethality in mice lacking keratin 8. Genes Dev. *7*, 1191–1202.

Bianchi, R., Giambanco, I., and Donato, R. (1993). S-100 protein, but not calmodulin, binds to the glial fibrillary acidic protein and inhibits

its polymerization in a Ca^{2+}-dependent manner. J. Biol. Chem. *268*, 12669–12674.

Bradley, A. (1987). Production and analysis of chimaeric mice. In Teratocarcinomas and Embryonic Stem Cells: A Practical Approach, E. J. Robertson, ed. (Oxford: IRL press), pp. 113–151.

Brown, H. R., Goller, N. L., Rudelli, R. D., Merz, G. S., Wolfe, G. C., Wisniewski, H. M., and Robakis, N. K. (1990). The mRNA encoding the scrapie agent protein is present in a variety of non-neuronal cells. Acta Neuropathol. *80*, 1–6.

Büeler, H., Aguzzi, A., Sailer, A., Greiner, R.-A., Autenried, P., Aguet, M., and Weissmann, C. (1993). Mice devoid of PrP are resistant to scrapie. Cell *73*, 1339–1347.

Capecchi, M. R. (1989). Altering the genome by homologous recombination. Science *244*, 1288–1292.

Carlson, G. A., Goodman, P. A., Lovett, M., Taylor, B. A., Marshall, S. T., Peterson-Torchia, M., Westaway, D., and Prusiner, S. B. (1988). Genetics and polymorphism of the mouse prion gene complex: control of scrapie incubation time. Mol. Cell. Biol. *8*, 5528–5540.

Cashman, N. R., Loertscher, R., Nalbantoglu, J., Shaw, I., Kascsak, R. J., Bolton, D. C., and Bendheim, P. E. (1990). Cellular isoform of the scrapie agent protein participates in lymphocyte activation. Cell *61*, 185–192.

Chiu, F.-C., Barnes, E. A., Das, K., Haley, J., Socolow, P., Macaluso, F. P., and Fant, J. (1989). Characterization of a novel 66 kd subunit of mammalian neurofilaments. Neuron *2*, 1435–1445.

Colucci-Guyon, E., Portier, M.-M., Dunia, I., Paulin, D., Pournin, S., and Babinet, C. (1994). Mice lacking vimentin develop and reproduce without an obvious phenotype. Cell *79*, 679–694.

Collinge, J., Whittington, M. A., Sidle, K. C. L., Smith, C. J., Palmer, M. S., Clarke, A. R., and Jefferys, J. G. R. (1994). Prion protein is necessary for normal synaptic function. Nature *370*, 295–297.

Dahl, D., Bignami, A., Weber, K., and Osborn, M. (1981). Filament proteins in rat optic nerves undergoing wallerian degeneration: localization of vimentin, the fibroblast 100-Å filament protein, in normal and reactive astrocytes. Exp. Neurol. *73*, 496–506.

DeArmond, S. J., Mobley, W. C., DeMott, D. L., Barry, R. A., Beckstead, J. H., and Prusiner, S. B. (1987). Changes in the localization of brain prion proteins during scrapie infection. Neurology *37*, 1271–1280.

Diedrich, J. F., Bendheim, P. E., Kim, Y. S., Carp, R. I., and Haase, A. T. (1991). Scrapie-associated prion protein accumulates in astrocytes during scrapie infection. Proc. Natl. Acad. Sci. USA *88*, 375–379.

Eng, L. F. (1988). Astrocytic response in injury. In Current Issues in Neural Regeneration Research, P. J. Reier, R. P. Bunge, and F. J. Seil, eds. (New York: Alan R. Liss), pp. 247–255.

Fliegner, K. H., and Liem, R. K. H. (1991). Cellular and molecular biology of neuronal intermediate filaments. Int. Rev. Cytol. *131*, 109–167.

Franko, M. C., Gibbs, C. J., Jr., Rhoades, D. A., and Gajdusek, C. (1987). Monoclonal antibody analysis of keratin expression in the central nervous system. Proc. Natl. Acad. Sci. USA *84*, 3482–3485.

Frederiksen, K., and McKay, R. (1988). Proliferation and differentiation of rat neuroepithelial precursor cells in vivo. J. Neurosci. *8*, 1144–1151.

Hilmert, H., and Diringer, H. (1984). A rapid efficient method to enrich SAF-protein from scrapie brains of hamsters. Biosci. Rep. *4*, 165–170.

Hirano, A., Ghatak, N. R., Johnson, A. B., Partnow, M. J., and Gomori, A. J. (1972). Argentophilic plaques in Creutzfeldt–Jakob disease. Arch. Neurol. *26*, 530–542.

Hockfield, S., and McKay, R. (1985). Identification of major cell classes in the developing mammalian nervous system. J. Neurosci. *5*, 3310–3328.

Hooper, M., Hardy, K., Handyside, A., Hunter, S., and Monk, M. (1987). HPRT-deficient (Lesch–Nyhan) mouse embryos derived from germline colonization by cultured cells. Nature *326*, 292–295.

Itohara, S., Mombaerts, P., Lafaille, J., Iacomini, J., Nelson, A., Clarke, A. R., Hooper, M. L., Farr, A., and Tonegawa, S. (1993). T cell receptor δ gene mutant mice: independent generation of αβ T cells and programmed rearrangements of γδ TCR genes. Cell *72*, 337–348.

Janzer, R. C., and Raff, M. C. (1987). Astrocytes induce blood-brain barrier properties in endothelial cells. Nature *325*, 253–257.

Klymkowsky, M. W., Miller, R. H., and Lane, E. B. (1983). Morphology, behavior, and interaction of cultured epithelial cells after the antibody-induced disruption of keratin filament organization. J. Cell Biol. *96*, 494–509.

Kocisko, D. A., Come, J. H., Priola, S. A., Chesebro, B., Raymond, G. J., Lansbury, P. T., and Caughey, B. (1994). Cell-free formation of protease-resistant prion protein. Nature *370*, 471–474.

Kretzschmar, H. A., Prusiner, S. B., Stowring, L. E., and DeArmond, S. J. (1986). Scrapie prion proteins are synthesized in neurons. Am. J. Pathol. *122*, 1–5.

Laemmli, U. K. (1970). Cleavage of structural proteins during the assembly of the head of bacteriophage T4. Nature *227*, 680–685.

Liem, R. K. H. (1993). Molecular biology of neuronal intermediate filaments. Curr. Opin. Cell Biol. *5*, 12–16.

Lendahl, U., Zimmerman, L. B., and McKay, R. D. G. (1990). CNS stem cells express a new class of intermediate filament protein. Cell *60*, 585–595.

Ludwin, S. K., Kosek, J. C., and Eng, L. F. (1976). The topographical distribution of S-100 and GFA proteins in the adult rat brain: an immunohistochemical study using horseradish peroxidase–labelled antibodies. J. Comp. Neurol. *165*, 197–207.

Mackenzie, A. (1983). Immunohistochemical demonstration of glial fibrillary acidic protein in scrapie. J. Comp. Pathol. *93*, 251–259.

Manuelidis, L., Tesin, D. M., Sklaviadis, T., and Manuelidis, E. E. (1987). Astrocyte gene expression in Creutzfeldt–Jakob disease. Proc. Natl. Acad. Sci. USA *84*, 5937–5941.

McBurney, M. W., Sutherland, L. C., Adra, C. N., Leclair, B., Rudnicki, M. A., and Jardine, K. (1991). The mouse *Pgk-1* gene promoter contains an upstream activator sequence. Nucl. Acids Res. *19*, 5755–5761.

Norenberg, M. D. (1994). Astrocyte responses to CNS injury. J. Neuropathol. Exp. Neurol. *53*, 213–220.

Oesch, B., Teplow, D. B., Stahl, N., Serban, D., Hood, L. E., and Prusiner, S. B. (1990). Identification of cellular proteins binding to the scrapie prion protein. Biochemistry *29*, 5848–5855.

Peters, A., Palay, S. L., and Webster, H. de F. (1991). The Fine Structure of the Nervous System: Neurons and Their Supporting Cells, 3rd edition (New York: Oxford University Press).

Petito, C. K., Morgello, S., Felix, J. C., and Lesser, M. L. (1990). The two patterns of reactive astrocytosis in postischemic rat brain. J. Cereb. Blood Flow Metab. *10*, 850–859.

Pixley, S. K. R., and de Vellis, J. (1984). Transition between immature radial glia and mature astrocytes studied with a monoclonal antibody to vimentin. Dev. Brain Res. *15*, 201–209.

Pixley, S. K. R., Kobayashi, Y., and de Vellis, J. (1984). A monoclonal antibody against vimentin: characterization. Dev. Brain Res. *15*, 185–199.

Prusiner, S. B. (1982). Novel proteinaceous infectious particles cause scrapie. Science *216*, 136–143.

Prusiner, S. B. (1991). Molecular biology of prion diseases. Science *252*, 1515–1522.

Prusiner, S. B., Cochran, S. P., Groth, D. H., Downey, D. E., Bowman, K. A., and Martinez, H. M. (1982). Measurement of the scrapie agent using an incubation time interval assay. Ann. Neurol. *11*, 353–358.

Pruss, R. M., Mirsky, R., and Raff, M. C. (1981). All classes of intermediate filaments share a common antigenic determinant defined by a monoclonal antibody. Cell *27*, 419–428.

Quinlan, R. A., and Franke, W. W. (1983). Molecular interactions in intermediate-sized filaments revealed by chemical cross-linking. Eur. J. Biochem. *132*, 477–484.

Rakic, P. (1972). Mode of cell migration to the superficial layers of fetal monkey neocortex. J. Comp. Neurol. *145*, 61–83.

Rakic, P. (1981). Neuronal–glial interaction during brain development. Trends Neurosci. *4*, 184–187.

Reese, T. S., and Karnovsky, M. J. (1967). Fine structural localization of a blood-brain barrier to exogenous peroxidase. J. Cell Biol. *34*, 207–217.

Reier, P. J., and Houle, J. D. (1988). The glial scar: its bearing on axonal elongation and transplantation approaches to CNS repair. In Physiological Basis for Functional Recovery in Neurological Disease, S. D. Waxman, ed. (New York: Raven Press), pp. 87–138.

Sapirstein, V. S. (1983). Development of membrane-bound carbonic anhydrase and glial fibrillary acidic protein in normal and quaking mice. Dev. Brain Res. *6*, 13–19.

Schiffer, D., Giordana, M. T., Migheli, A., Giaccone, G., Pezzotta, S., and Mauro, A. (1986). Glial fibrillary acidic protein and vimentin in the experimental glial reaction of the rat brain. Brain Res. *374*, 110–118.

Schmechel, D. E., and Rakic, P. (1979). A golgi study of radial glial cells in developing monkey telencephalon: morphogenesis and transformation into astrocytes. Anat. Embryol. *156*, 115–152.

Schnitzer, J., Franke, W. W., and Schachner, M. (1981). Immunocytochemical demonstration of vimentin in astrocytes and ependymal cells of developing and adult mouse nervous system. J. Cell Biol. *90*, 435–447.

Shinagawa, M., Takahashi, K., Sasaki, S., Doi, S., Goto, H., and Sato, G. (1985). Characterization of scrapie agent isolated from sheep in Japan. Microbiol. Immunol. *29*, 543–551.

Steinert, P. M., and Roop, D. R. (1988). Molecular and cellular biology of intermediate filaments. Annu. Rev. Biochem. *57*, 593–625.

Szaro, B. G., Grant, P., Lee, V. M.-Y., and Gainer, H. (1991). Inhibition of axonal development after injection of neurofilament antibodies into a *Xenopus laevis* embryo. J. Comp. Neurol. *308*, 576–585.

Torpey, N., Wylie, C. C., and Heasman, J. (1992). Function of maternal cytokeratin in Xenopus development. Nature *357*, 413–415.

Vassar, R., Coulombe, P. A., Degenstein, L., Albers, K., and Fuchs, E. (1991). Mutant keratin expression in transgenic mice causes marked abnormalities resembling a human genetic skin disease. Cell *64*, 365–380.

Wang, E., Cairncross, J. G., and Liem, R. K. H. (1984). Identification of glial filament protein and vimentin in the same intermediate filament system in human glioma cells. Proc. Natl. Acad. Sci. USA *81*, 2102–2106.

Weinstein, D. E., Shelanski, M. L., and Liem, R. K. H. (1991). Suppression by antisense mRNA demonstrates a requirement for the glial fibrillary acidic protein in the formation of stable astrocytic processes in response to neurons. J. Cell Biol. *112*, 1205–1213.

Weir, M. D., Patel, A. J., Hunt, A., and Thomas, D. G. T. (1984). Developmental changes in the amount of glial fibrillary acidic protein in three regions of the rat brain. Dev. Brain Res. *15*, 147–154.

Wietgrefe, S., Zupancic, M., Haase, A., Chesebro, B., Race, R., Frey, W., II, Rustan, T., and Friedman, R. L. (1985). Cloning of a gene whose expressions is increased in scrapie and senile plaques in human brain. Science *230*, 1177–1179.

Xu, Z., Cork, L. C., Griffin, J. W., and Cleveland, D. W. (1993). Increased expression of neurofilament subunit NF-L produces morphological alterations that resemble the pathology of human motor neuron disease. Cell *73*, 23–33.

Yagi, T., Ikawa, Y., Yoshida, K., Shigetani, Y., Takeda, N., Mabuchi, I., Yamamoto, T., and Aizawa, S. (1990). Homologous recombination at *c-fyn* locus of mouse embryonic stem cells with use of diphtheria toxin A-fragment gene in negative selection. Proc. Natl. Acad. Sci. USA *87*, 9918–9922.

Yamasaki, H., Itakura, C., and Mizutani, M. (1991). Hereditary hypotrophic axonopathy with neurofilament deficiency in a mutant strain of the Japanese quail. Acta Neuropathol. *82*, 427–434.

Yokoyama, K., Mori, H., and Kurokawa, M. (1981). Astroglial filament and fibroblast intermediate filament proteins in cytoskeletal preparations from spinal cord and optic nerve. FEBS Lett. *135*, 25–30.